





Cite this: *Phys. Chem. Chem. Phys.*,  
2024, 26, 1364

## H<sub>2</sub> formation from the E<sub>2</sub>–E<sub>4</sub> states of nitrogenase†

Hao Jiang  and Ulf Ryde \*

Nitrogenase is the only enzyme that can cleave the strong triple bond in N<sub>2</sub>, making nitrogen available for biological lifeforms. The active site is a MoFe<sub>7</sub>S<sub>9</sub>C cluster (the FeMo cluster) that binds eight electrons and protons during one catalytic cycle, giving rise to eight intermediate states E<sub>0</sub>–E<sub>7</sub>. It is experimentally known that N<sub>2</sub> binds to the E<sub>4</sub> state and that H<sub>2</sub> is a compulsory byproduct of the reaction. However, formation of H<sub>2</sub> is also an unproductive side reaction that should be avoided, especially in the early steps of the reaction mechanism (E<sub>2</sub> and E<sub>3</sub>). Here, we study the formation of H<sub>2</sub> for various structural interpretations of the E<sub>2</sub>–E<sub>4</sub> states using combined quantum mechanical and molecular mechanical (QM/MM) calculations and four different density-functional theory methods. We find large differences in the predictions of the different methods. B3LYP strongly favours protonation of the central carbide ion and H<sub>2</sub> cannot form from such structures. On the other hand, with TPSS, r<sup>2</sup>SCAN and TPSSh, H<sub>2</sub> formation is strongly exothermic for all structures and E<sub>n</sub> and therefore need strict kinetic control to be avoided. For the E<sub>2</sub> state, the kinetic barriers for the low-energy structures are high enough to avoid H<sub>2</sub> formation. However, for both the E<sub>3</sub> and E<sub>4</sub> states, all three methods predict that the best structure has two hydride ions bridging the same pair of Fe ions (Fe2 and Fe6) and these two ions can combine to form H<sub>2</sub> with an activation barrier of only 29–57 kJ mol<sup>−1</sup>, corresponding to rates of 7 × 10<sup>2</sup> to 5 × 10<sup>7</sup> s<sup>−1</sup>, *i.e.* much faster than the turnover rate of the enzyme (1–5 s<sup>−1</sup>). We have also studied H-atom movements within the FeMo cluster, showing that the various protonation states can quite freely be interconverted (activation barriers of 12–69 kJ mol<sup>−1</sup>).

Received 25th October 2023,  
Accepted 5th December 2023

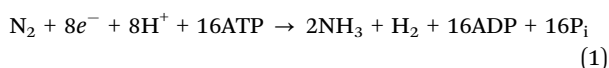
DOI: 10.1039/d3cp05181a

rsc.li/pccp

## Introduction

Nitrogenase (EC 1.18/19.6.1) is the only enzyme that can cleave the strong triple bond in N<sub>2</sub>, making atmospheric nitrogen available to plant life.<sup>1–4</sup> Crystallographic studies have shown that the most active type of nitrogenase contains a MoFe<sub>7</sub>S<sub>9</sub>C(homocitrate) cofactor in the active site, called the FeMo cluster.<sup>5–9</sup>

Nitrogenase catalyses the chemical reaction<sup>3,4</sup>



showing that eight electrons and protons are needed to convert N<sub>2</sub> to two molecules of ammonia. Consequently, the reaction is typically described by eight intermediates E<sub>0</sub>–E<sub>7</sub>, differing in the number of added electrons and protons.<sup>10</sup> It has been shown that the enzyme needs to be loaded by four electrons and protons (*i.e.* to E<sub>4</sub>) before N<sub>2</sub> can bind.<sup>3,4</sup> It is currently

believed that the binding of N<sub>2</sub> is promoted by the dissociation of H<sub>2</sub>, which is formed by reductive elimination of two hydride ions that bridge two Fe ions each.<sup>11–15</sup> This explains why H<sub>2</sub> is a compulsory byproduct in the reaction mechanism (*cf.* eqn (1)).

In spite of numerous spectroscopic, kinetic, biochemical and computational studies,<sup>1–9,16,17</sup> many details of the reaction mechanism of nitrogenase are still unknown.<sup>4,17</sup> An important reason for this is that different density-functional theory (DFT) methods give widely different predictions of the relative stability of various models of the active site of nitrogenase, *e.g.* different protonation states of the E<sub>n</sub> states.<sup>17–20</sup>

The structure of the resting E<sub>0</sub> state is well-known from accurate crystal structures, and combined quantum mechanical and molecular mechanical (QM/MM) calculations.<sup>4,5,21–23</sup> Moreover, quantum refinement has shown that this state does not contain any extra protons.<sup>20</sup> For the singly reduced and protonated E<sub>1</sub> state, DFT studies and EXAFS measurements indicate that one of the μ<sub>2</sub> bridging sulfide ions, S2B (atom names are shown in Fig. 1), is protonated.<sup>20,24–26</sup> However, spectroscopic studies of Fe-nitrogenase (in which the Mo ions is replaced by Fe), indicate that it instead should contain a dissociable hydride ions,<sup>27</sup> although this is not supported by recent QM/MM calculations.<sup>28</sup>

Department of Computational Chemistry, Lund University, Chemical Centre, P. O. Box 124, SE-221 00 Lund, Sweden. E-mail: Ulf.Ryde@compchem.lu.se;  
Fax: +46 2228648; Tel: +46 2224502

† Electronic supplementary information (ESI) available. See DOI: <https://doi.org/10.1039/d3cp05181a>



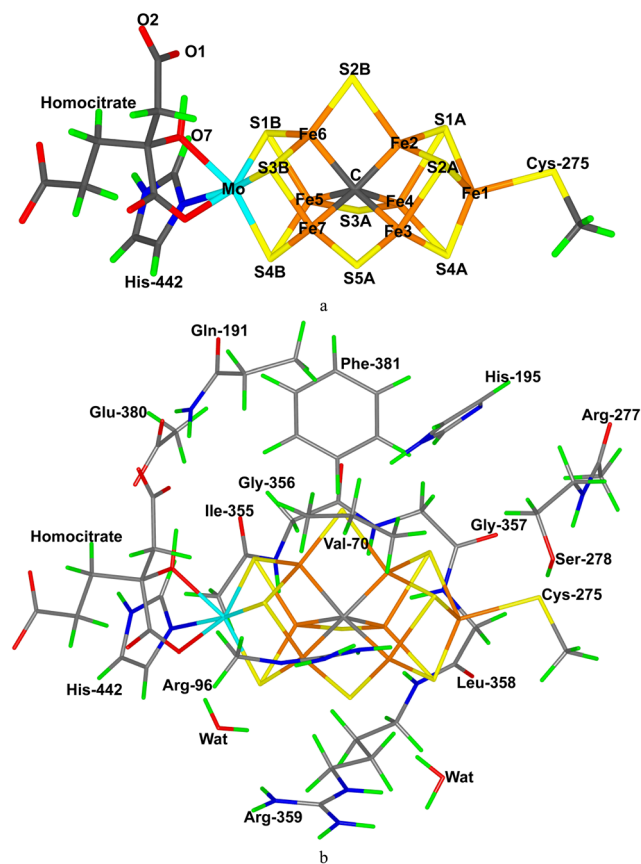


Fig. 1 (a) The FeMo cluster of nitrogenase, showing also the atom names. (b) The QM system used in the calculations, showing the names of the surrounding residues.

For the  $E_2$  state, the results with different DFT methods start to differ.<sup>20</sup> Calculations with the pure meta generalised gradient approximation (mGGA) functional TPSS<sup>29</sup> suggest that the best structure involves a proton on S2B and a hydride ion bridging the Fe2 and Fe6 ions.<sup>19</sup> Other mGGA or hybrid functionals with a low amount of Hartree–Fock (HF) exchange ( $r^2$ SCAN<sup>30</sup> and TPSSh<sup>31</sup>) suggest a similar structure, but with the protonated S2B ion dissociated from one of the Fe ions.<sup>32</sup> A structure with both S2B and S5A protonated is also competitive with TPSSh.<sup>33</sup> The hybrid B3LYP functional (with 20% HF exchange)<sup>34–36</sup> suggests instead that the central carbide ion is doubly protonated. Likewise, for the  $E_3$  state B3LYP suggests a structure with a triply protonated carbide ions, whereas the other functionals suggest a structure with S2B protonated and dissociated from one Fe ion, and two hydride ions both bridging between the Fe2 and Fe6 ions.<sup>32</sup> Other structures with a terminal hydride ion or a bound  $H_2$  molecule have also been proposed.<sup>37</sup>

For the key  $E_4$  intermediate, many different structures have been suggested.<sup>17</sup> ENDOR experiments show that  $E_4$  should contain two bridging hydride ions<sup>12,13,15</sup> and based on this and computational studies, Hoffman and coworkers have suggested a structure in which S2B and S5A are protonated and there are two hydride ions bridging the Fe2/6 and the Fe3/7 pairs of ions,

with all H atoms pointing towards the same face of the FeMo cluster.<sup>38</sup> We made a systematic search of structures with two bridging hydride ions and showed that a structure with the protons and the hydride ions at the same positions is most stable, but three of them were pointing towards other faces of the FeMo cluster.<sup>39</sup> On the other hand, Bjornsson and coworkers have advocated for structures in which the two hydride ions both bridge Fe2/6, S2B is protonated and dissociated from one Fe and the second proton is on S5A.<sup>40</sup> A thorough study of many of these structures indicated that with TPSS, the Hoffman and Bjornsson-type structures are nearly degenerate, whereas the latter are most stable with  $r^2$ SCAN and TPSSh.<sup>32</sup> A structure with a triply protonated carbide ion and the fourth proton on S2B is by far best by B3LYP (and competitive with TPSSh).<sup>41,42</sup> It has also been suggested that S2B may fully dissociate from the FeMo cluster,<sup>43–46</sup> inspired by crystallographic studies showing lability of this ligand.<sup>8,47,48</sup>

Recently, we studied the binding of  $N_2$  to the  $E_0$ – $E_4$  states of nitrogenase and showed that only the TPSS<sup>29</sup> functional gave binding energies in accordance with experiments (*i.e.* a favourable binding to  $E_3$  and  $E_4$ ), but not to  $E_0$ – $E_2$ .<sup>32</sup> The other tested functionals gave too weak binding to  $E_3$  or  $E_4$ . Other studies have suggested stronger binding of  $N_2$ , but this depends on how the binding energy is defined and how the entropy loss of the  $N_2$  ligand is treated.<sup>40,49–51</sup>

A related question is the formation and dissociation of  $H_2$  from the FeMo cluster. This is a very important reaction. If  $H_2$  forms from the  $E_2$  and  $E_3$  states of nitrogenase, the enzyme goes back to the  $E_0$  and  $E_1$  states, respectively, and two electrons and protons have been lost on an unproductive side reaction.<sup>4,33</sup> On the other hand, formation of  $H_2$  is desirable for the  $E_4$  state, but only if it is directly coupled to the binding of  $N_2$ .

Khadka and coworkers have studied  $H_2$  evolution from the  $E_2$  state with mediated bioelectrocatalysis and DFT calculations.<sup>52</sup> The experiments showed that the rate-limiting step for  $H_2$  formation is hydride protonation. The calculations were performed with a minimal QM model of the active site in a continuum solvent. They were started from a structure with S2B protonated and a hydride ion bridging Fe2 and Fe6. A free-energy barrier of only 29 kJ mol<sup>−1</sup> was obtained.

Thorhallsson and Bjornsson have studied the formation of  $H_2$  from the  $E_2$  state of nitrogenase by QM/MM calculations.<sup>33</sup> They found activation barriers of 86–95 kJ mol<sup>−1</sup> from a structure with S2B dissociated from one of the Fe ions, depending on the protonation state of the nearby His-195 residue. Interestingly, the barrier was much lower (48 kJ mol<sup>−1</sup>) when calculated with a small QM-cluster model, indicating that the surrounding protein counteracts this side reaction.

Here, we extend these investigations by studying the formation and dissociation of  $H_2$  from the FeMo cluster in the  $E_2$ – $E_4$  states. The aim of this investigation is three-fold: The first is to study the  $H_2$ -formation reaction for many different structures: combining either two hydride ions or one proton and one hydride ion, and studying reactions for different positions in the cluster, *e.g.* both terminal and bridging hydride ions, located on different Fe ions or on the same Fe ion. The second is to study how easily different



protonation states can be interconverted. This may answer the question whether the enzyme can avoid the formation of  $H_2$  by posing the proton and hydride ions far from each other. The third is to compare the results of four different DFT functionals. We know that the enzyme needs to avoid the loss of  $H_2$  from the  $E_2$  and  $E_3$  states, whereas  $H_2$  formation is necessary for the  $E_4$  state, but only in conjunction with the binding of  $N_2$ . If the  $H_2$  formation is too facile for the  $E_2$  and  $E_3$  states, it is an indication of problems with the DFT method used or that the proper structure is still not found.

## Methods

### The protein

The calculations were based on the 1.0 Å crystal structure of Mo nitrogenase from *Azotobacter vinelandii* (PDB code 3U7Q).<sup>5</sup> The setup of the protein is identical to that of our previous studies.<sup>18,32,39,53</sup> The entire heterotetramer was included in the calculations and the quantum mechanical (QM) calculations were concentrated on the FeMo clusters in the C subunit because there is a buried imidazole molecule rather close to the active site ( $\sim 11$  Å) in the A subunit. The two P clusters and the FeMo cluster in subunit A were modelled by MM in the fully reduced and resting states, respectively, using a QM charge model.<sup>53</sup> The protonation states of all residues were the same as before,<sup>53</sup> and the homocitrate ligand was modelled in the singly protonated state with a proton shared between the hydroxyl group (O7 that coordinates to Mo) and the O1 carboxylate atom.<sup>23,53</sup> The protein was solvated in a sphere with a radius of 65 Å around the geometrical centre of the protein.  $Cl^-$  and  $Na^+$  ions were added to an ionic strength of 0.2 M.<sup>54</sup> The final system contained 133 915 atoms. For the protein, we used the Amber ff14SB force field<sup>55</sup> and water molecules were described by the TIP3P model.<sup>56</sup> The metal sites were treated by a non-bonded model<sup>57</sup> and charges were obtained with the restrained electrostatic potential method.<sup>58</sup>

The FeMo cluster was modelled by  $MoFe_7S_9C(\text{homocitrate})-(CH_3S)(\text{imidazole})$ , where the two last groups are models of Cys-275 and His-442. In addition, all groups that form hydrogen bonds to the FeMo cluster were also included in the QM model, viz. Arg-96, Gln-191 and His-195 (sidechains), Ser-278 and Arg-359 (both backbone and sidechain, including the CA and C and O atoms from Arg-277), Gly-356, Gly-357 and Leu-358 (backbone, including the CA and C and O atoms from Ile-355), as well as two water molecules. Finally, the sidechain of Glu-380 was included because it forms hydrogen bonds to Gln191 and His-442, as well as the sidechains of Val-70 and Phe-381 because they are close to S2B, Fe2 and Fe6, i.e. the expected reactive site. The QM system contained 191–193 atoms depending on the  $E_n$  state and is shown in Fig. 1. The net charge of QM region was  $-4 e$ .

### QM calculations

All QM calculations were performed with the Turbomole software (versions 7.5 and 7.6).<sup>59</sup> All structures were studied with

the TPSS,<sup>29</sup>  $r^2\text{SCAN}$ ,<sup>30</sup> TPSSh<sup>31</sup> and B3LYP<sup>34–36</sup> functionals, whereas reactions were primarily studied with the TPSS and TPSSh functionals. TPSS and  $r^2\text{SCAN}$  are mGGA functionals, whereas TPSSh and B3LYP are hybrid functionals with 10 and 20% HF exchange, respectively. TPSS has been used in most of our previous studies of nitrogenase<sup>20,39,53,60</sup> and gives the best  $N_2$  binding energies.<sup>32</sup>  $r^2\text{SCAN}$  and TPSSh have been shown to give accurate structures of nitrogenase models.<sup>61</sup> All calculations involved the def2-SV(P) basis set.<sup>62</sup> The calculations were sped up by expanding the Coulomb interactions in an auxiliary basis set, the resolution-of-identity (RI) approximation.<sup>63,64</sup> Empirical dispersion corrections were included with the DFT-D4 approach,<sup>65</sup> as implemented in Turbomole.

In this investigation we study the  $E_0$ – $E_4$  states of the FeMo cluster. The resting  $E_0$  state has the formal  $Mo^{III}Fe^{II}_3Fe^{III}_4$  oxidation state<sup>21,23,66</sup> and is a quartet state according to experiments.<sup>4</sup> The other four states were obtained by successively adding one electron and one proton to the previous state. Several positions of the added protons were tested, based on previous investigations,<sup>32</sup> as will be discussed below.  $E_2$  was studied in the quartet spin state and  $E_4$  in the doublet state, in agreement with experiments<sup>1–4,67–69</sup> For  $E_1$  and  $E_3$ , no experimental data are available and we assumed the quintet and triplet states, respectively (previous studies have shown that different spin states are close in energy).<sup>19,20</sup>

The electronic structure of all QM calculations was obtained with the broken-symmetry (BS) approach.<sup>70</sup> Each of the seven Fe ions was modelled in the high-spin state, with either a surplus of  $\alpha$  (four Fe ions) or  $\beta$  (three Fe ions) spin. Such a state can be selected in 35 different ways.<sup>71</sup> The various BS states were obtained either by swapping the coordinates of the Fe ions<sup>72</sup> or with the fragment approach by Szilagy and Winslow.<sup>73</sup> The BS states are named by listing the numbers of the three Fe ions with minority spin, e.g. BS-235. The selection of the BS states was based on our previous experience with the similar systems.<sup>19,20,32,39,71,74</sup>

For the  $H_2$  dissociation energies ( $\Delta E_{H_2}$ ),  $H_2$  was optimised in a conductor-like screening model (COSMO)<sup>75,76</sup> continuum solvent with a dielectric constant of 80. These calculations employed the default optimised COSMO atomic radius for H (1.30 Å) and a water solvent radius of 1.3 Å.<sup>77</sup> The COSMO solvation energy of  $H_2$  is small, 1–3 kJ mol<sup>-1</sup>, making this energy correction insignificant.

### QM/MM calculations

QM/MM calculations were performed with the ComQum software.<sup>78,79</sup> In this approach, the protein and solvent are split into three subsystems: system 1 (the QM region) was relaxed by QM methods. System 2 was kept fixed at the original coordinates (equilibrated crystal structure), to avoid the risk that different calculations end up in different local minima.

In the QM calculations, system 1 was represented by a wavefunction, whereas all the other atoms were represented by an array of partial point charges, one for each atom, taken from the MM setup. Thereby, the polarisation of the QM system by the surroundings is included in a self-consistent manner. When there is a bond between systems 1 and 2 (a junction), the hydrogen link-atom approach was employed: The QM system was capped with hydrogen atoms, the positions of which are



linearly related to the corresponding carbon atoms (carbon link atoms, CL) in the full system.<sup>78,80</sup> All atoms were included in the point-charge model, except the CL atoms.<sup>81</sup> ComQum employs a subtractive scheme with van der Waals link-atom corrections.<sup>82</sup> No cut-off is used for the QM and QM-MM interactions. The geometry optimisations were continued until the energy change between two iterations was less than  $2.6 \text{ J mol}^{-1}$  ( $10^{-6}$  a.u.) and the maximum norm of the Cartesian gradients was below  $10^{-3}$  a.u. Approximate transition states for the formation of  $\text{H}_2$  were obtained by performing relaxed scans of H–H distances.

## Result and discussion

We have studied the formation of  $\text{H}_2$  in nitrogenase. This is not possible until the  $\text{E}_2$  state when two protons have accumulated on the cluster. Therefore, we have studied the  $\text{E}_2\text{--E}_4$  states. The results at each reduction level are discussed in separate sections. We also study proton transfers within the FeMo cluster, connecting the various protonated structures.

### $\text{H}_2$ formation in the $\text{E}_2$ state

We first studied the formation and dissociation of  $\text{H}_2$  from the  $\text{E}_2$  state. As discussed in the Introduction, different DFT functionals give different predictions of what is the most stable structure (protonation) of the  $\text{E}_2$  state. Based on previous investigations,<sup>19,32</sup> we have studied  $\text{H}_2$  formation and proton transfers within seven structural candidates for the  $\text{E}_2$  state. These and some additional low-energy structural candidates are shown in Fig. 2. Relative energies calculated with four DFT functionals are shown in Table 1.

With the TPSS functional, the most stable structures have one proton bound to S2B (which bridges Fe2 and Fe6, *cf.* Fig. 1) and one hydride ion also bridging Fe2 and Fe6. There are four structural isomers of this structure depending on the direction of the two H atoms. The best one has the hydride ion on the same side of S2B as S3B (called Fe2/6(3)) and the proton on S2B also points towards S3A (called S2B(3)). This is structure B33 in Fig. 2 (“B” because both S2B and the hydride ion bridge Fe2 and Fe6). The other three isomers are called B35, B53 and B55, depending on whether the proton on S2B points towards S3A or

S5A (first number) and whether the hydride ion is on the same side of S2B as S3A or S5A (second number). They are  $4\text{--}33 \text{ kJ mol}^{-1}$  less stable than the B33 structure with TPSS.

For the B33 structure, the proton and the hydride ion are both on the same side of the cluster, with a distance of  $2.32\text{--}2.33 \text{ \AA}$  in the optimised structures, and therefore the formation of  $\text{H}_2$  from these two atoms is quite straight forward. The transition state is late, at a H–H distance of  $1.0\text{--}1.1 \text{ \AA}$ , and the barrier is  $86\text{--}91 \text{ kJ mol}^{-1}$  (calculated with TPSS or TPSSh). For the B55 structure, the hydride ion and the proton are also on the same side of the cluster, at a distance of  $2.21\text{--}2.23 \text{ \AA}$ . However, for this structure, the activation energy for  $\text{H}_2$  formation is lower,  $51\text{--}55 \text{ kJ mol}^{-1}$ .

For the other two structures (B35 and B53), the proton and the hydride ion are on different sides of the cluster, with initial distances of  $3.4\text{--}3.5 \text{ \AA}$ . Therefore, the reaction has to be performed in two steps. For example, B35 could first be isomerised to B33 by a rotation of the proton on S2B to the other side and then the transfer of the proton to the Fe2/6 hydride ion (which we have already studied). The rotation has a barrier of  $55\text{--}62 \text{ kJ mol}^{-1}$ .

With TPSSh and  $\text{r}^2\text{SCAN}$ , the best structure still has a proton on S2B and a hydride ion bridging Fe2/6, but S2B has dissociated from Fe2, but not from Fe6. This structure is called H6 in Fig. 2, indicating that S2B is half-dissociated, still binding to Fe6. The corresponding structure with S2B dissociated from Fe6 instead ( $\text{H}_2$  in Fig. 2) is  $71\text{--}97 \text{ kJ mol}^{-1}$  higher in energy. With TPSS, B33 is  $13 \text{ kJ mol}^{-1}$  more stable than H6, whereas the opposite is true with  $\text{r}^2\text{SCAN}$  and TPSSh by  $41$  and  $14 \text{ kJ mol}^{-1}$ , respectively.

For the H6 structure, the two H atoms are also on the same side of the cluster, with a distance of  $2.43\text{--}2.48 \text{ \AA}$ . However, the activation barrier for  $\text{H}_2$  formation is quite high,  $79 \text{ kJ mol}^{-1}$  with TPSS and  $104 \text{ kJ mol}^{-1}$  with TPSSh. The transition state has a H–H distance of  $1.0\text{--}1.1 \text{ \AA}$ . For this structure, we also studied how easily the proton on the half-dissociated S2B ion may rotate  $360^\circ$  around the Fe6–S2B axis. We found two local minima. The lowest is that shown in Fig. 2, with the proton pointing between the hydride ion and S1B. In the second, which is  $2\text{--}3 \text{ kJ mol}^{-1}$  less stable, it instead points towards S3B. The two minima are separated by barriers of only  $12\text{--}17 \text{ kJ mol}^{-1}$ . Thus, the rotation of this proton is essentially free and it is enough to study the most stable structure.

Moreover, we studied the formation of H6 from B33 by cleavage of the S2B–Fe2 bond. This cleavage turned out to be quite facile, with a barrier of  $35\text{--}39 \text{ kJ mol}^{-1}$ . Similar reactions could also be used twice to move hydride ion in the B-type structures.

With B3LYP, the most stable structure instead has a doubly protonated central carbide ion. This structure is called C2 (two protons on the carbide ion). It is  $88 \text{ kJ mol}^{-1}$  more stable than the H6 state with B3LYP, whereas the opposite is true by  $66\text{--}155 \text{ kJ mol}^{-1}$  with the other functionals. We tried to form  $\text{H}_2$  in the C2 structure using the B3LYP functional. Interestingly, even if the two protons on the carbide ion are quite close ( $1.71 \text{ \AA}$ ), no reaction could be obtained; instead the energy increased monotonically to over  $200 \text{ kJ mol}^{-1}$  when the H–H

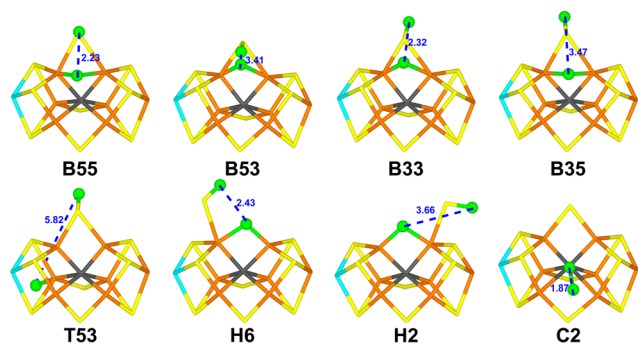


Fig. 2 The eight considered  $\text{E}_2$  structures, showing the structure obtained with TPSS (B3LYP for C2). The labels are explained in the text. H–H distances in  $\text{\AA}$  are marked in the figures.





**Table 1** Structures and reactions within the E<sub>2</sub> state, listing the structure (Struct), the positions of the two added H atoms (H1 and H2), the BS state, the H–H distance (Å), the relative energy ( $\Delta E$ ), the H<sub>2</sub> dissociation energy ( $\Delta E_{\text{H}_2}$ ) relative the E<sub>0</sub> state and H<sub>2</sub> in a COSMO solvent, and the activation energy for H<sub>2</sub> formation ( $\Delta E^\ddagger$ ; all energies in kJ mol<sup>−1</sup>)

Struct.	H1	H2	BS	TPSS				r <sup>2</sup> SCAN		TPSSh				B3LYP	
				H–H	$\Delta E$	$\Delta E_{\text{H}_2}$	$\Delta E^\ddagger$	$\Delta E$	$\Delta E_{\text{H}_2}$	H–H	$\Delta E$	$\Delta E_{\text{H}_2}$	$\Delta E^\ddagger$	$\Delta E$	$\Delta E_{\text{H}_2}$
B55	S2B(5)	Fe2/6(5)	235	2.23	33	−133	51	63	−166	2.21	42	−146	59	171	−158
B53	S2B(5)	Fe2/6(3)	235	3.41	4	−104		46	−150	3.45	21	−125	62	152	−139
B33	S2B(3)	Fe2/6(3)	235	2.32	0	−100	86	41	−145	2.33	14	−119	91	142 <sup>a</sup>	−130
B35	S2B(3)	Fe2/6(5)	235	3.47	17	−117		17	−120	3.55	9	−114		133	−120
T53	S2B(3)	Fe5	235	5.82	19	−119	160	25	−129	5.82	16	−120		115	−102
H6	S2B(H6)	Fe2/6	235	2.43	13	−113	79	0	−104	2.48	0	−104	104	88 <sup>a</sup>	−75
H2	S2B(H2)	Fe2/6	235	3.66	75	−175		80	−183	3.78	71	−175		186	−173
C2	C2367	C3457	345	1.87	155 <sup>b</sup>	−255		113	−217	1.77	35	−139		0 <sup>c</sup>	13
C1	S2B(3)	C2456	346	3.90										32	−18
E <sub>0</sub> + H <sub>2</sub> from B55				235	0.75	−57	−43	−60	−44	0.75	−65	−40		−32	−43
E <sub>0</sub> + H <sub>2</sub> from B33				235	0.75	−44	−56	−40	−64	0.76	−48	−57		−9	−66
E <sub>0</sub> + H <sub>2</sub> from H6S				235	0.76	−105	5	−109	5	0.76	−109	5		−82	6

<sup>a</sup> BS-346. <sup>b</sup> BS-235. <sup>c</sup>  $\Delta E^\ddagger > 220$  kJ mol<sup>−1</sup>.

distance was decreased. We also tried to move the Fe2/6 hydride ion in the H6S structure to the central carbide ion. However, the barrier for such a movement was quite high, 106 kJ mol<sup>−1</sup> with B3LYP. The product, which has protons on the carbide ion and on S2B (which rebound to Fe2 during the reaction) is 57 kJ mol<sup>−1</sup> more stable than the reactant and therefore only 32 kJ mol<sup>−1</sup> less stable than the C2 structure (*i.e.* the second-best structure with B3LYP; called C1 in Table 1).

Finally, we considered also H<sub>2</sub> formation from a structure with a hydride ion on Fe5 and a proton on S2B(3) (called T53, highlighting the terminal hydride ion). This structure is 16–25 kJ mol<sup>−1</sup> less stable than the best one for TPSS, r<sup>2</sup>SCAN and TPSSh (but 115 kJ mol<sup>−1</sup> with B3LYP). The distance between the two H atoms is 5.82 Å. Therefore, the hydride ion on Fe5, first has to move from the *exo* position (*trans* to C), to an *endo* position, where it almost bridges to Fe4. The barrier for this is quite low, only 32 kJ mol<sup>−1</sup>, and the intermediate is only 13 kJ mol<sup>−1</sup> less stable than the starting T53 structure. However, the reaction from this intermediate with a H–H distance of 3.6 Å has a barrier of 160 kJ mol<sup>−1</sup>, making the reaction prohibitive.

In all product structures of these reactions, the formed H<sub>2</sub> molecule has dissociated from the FeMo cluster. The structure of the cluster in these product states is similar because S2B binds back to Fe2 for the H6 structure, forming a normal E<sub>0</sub> structure. However, H<sub>2</sub> resides in different positions in the second coordination sphere. The most stable structure is the one starting from H6. In this structure, H<sub>2</sub> is 3.8 Å from Fe2 and it interacts weakly with His-195, Arg-277 and Ser-278 (*cf.* Fig. 3). This structure is 105–109 kJ mol<sup>−1</sup> more stable than the best E<sub>2</sub> structure with the TPSS, r<sup>2</sup>SCAN and TPSSh functionals, but it is 6 kJ mol<sup>−1</sup> less stable than the C2 structure with B3LYP. This shows that formation of H<sub>2</sub> is strongly downhill with the former three functionals.

Another way to quantify this is to calculate the energy difference between a certain structure and the E<sub>0</sub> state plus H<sub>2</sub> in water solution (optimised with the COSMO continuum-solvation model). This H<sub>2</sub> dissociation energy ( $\Delta E_{\text{H}_2}$ ) is given

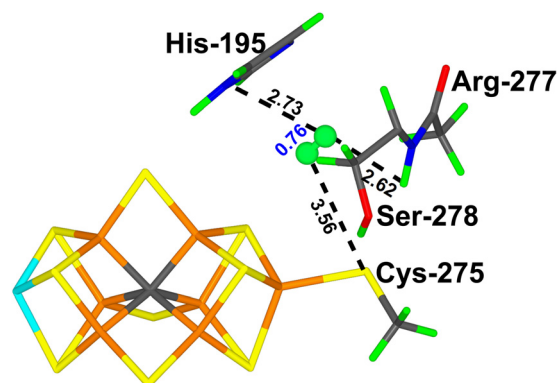


**Fig. 3** The best E<sub>2</sub> structure with H<sub>2</sub> in the second coordination sphere. The H–H bond length and distances to the nearest residues are marked (in Å).

for all structures in Table 1. It can be seen that formation and dissociation of H<sub>2</sub> are strongly favourable for all structures considered, by 100–255 kJ mol<sup>−1</sup> for TPSS, r<sup>2</sup>SCAN and TPSSh. For B3LYP, the energies are lower, and for the most stable C2 state, the H<sub>2</sub> dissociation energy is actually unfavourable by 13 kJ mol<sup>−1</sup>. Yet, H<sub>2</sub> dissociation would be further enhanced by translational and rotational entropy of the released H<sub>2</sub> molecule (typically estimated to 17–45 kJ mol<sup>−1</sup>).<sup>40,51,83,84</sup> For the three structures with H<sub>2</sub> already formed and located in the second coordination sphere,  $\Delta E_{\text{H}_2}$  is smaller and actually unfavourable by 5–6 kJ mol<sup>−1</sup> for the best structure with all four functionals (but again this will be reversed by the entropy term).

### H<sub>2</sub> dissociation from the E<sub>3</sub> state

Next, we studied H<sub>2</sub> formation from the E<sub>3</sub> state. As was discussed in the Introduction, the best E<sub>3</sub> structure with TPSS, r<sup>2</sup>SCAN and TPSSh has S2B protonated and dissociated from Fe2, but still binding to Fe6, and two hydride ions both bridging Fe2 and Fe6 (called structure S6, because the two hydride ions bind to the same pair of Fe ions and S2B binds to



Fe6; cf. Fig. 4). A structure with the proton on S2B pointing to another direction (towards S3B rather than S1B) is only 2–9 kJ mol<sup>-1</sup> less stable and since the results in the previous section indicated that the proton on the half-dissociated S2B may rotate quite freely around the Fe6–S2B axis, this structure is not further discussed. A structure with the proton and the hydride ions at the same positions, but with S2B binding to Fe2 instead (S2) is 52–85 kJ mol<sup>-1</sup> less stable than S6.

On the other hand, with B3LYP, a structure with a triply protonated carbide ion, is 195 kJ mol<sup>-1</sup> better (C3 in Fig. 4). With TPSS and r<sup>2</sup>SCAN, C3 is 141–189 kJ mol<sup>-1</sup> less stable than S6, but with TPSSh, the difference is only 4 kJ mol<sup>-1</sup>. We have studied several other E<sub>3</sub> structures, of two different types. One is related to Hoffman's suggestion for the E<sub>4</sub> state (*i.e.* with protons on S2B and S5A and hydride ions bridging Fe2/6 and Fe3/7), but missing one of the H atoms for E<sub>3</sub>.<sup>38</sup> They are named according to the direction of the four H atoms (towards, S3A, S2B or S5A), given by a number in the order S2B–Fe2/6–Fe3/7–S5A and with an underscore marking the missing H atom, *e.g.* 35\_2, (cf. Fig. 4). The second type has a proton on S2B(3) (which bridges Fe2/6), a terminal hydride on Fe5 and either another terminal hydride on Fe4 (called 345) or a hydride ion bridging Fe2/6, pointing either towards S3A or S5A (called 335 or 355, respectively; cf. Fig. 4). The best structures of these two types are 21–46 and 44–58 kJ mol<sup>-1</sup> less stable than the S6 structure (35\_3 and 355 best), respectively, with TPSS, r<sup>2</sup>SCAN and TPSSh, but 178 kJ mol<sup>-1</sup> worse than C3 with B3LYP (35\_2 best).

For all functionals, formation of H<sub>2</sub> is strongly exothermic, by 59–107 kJ mol<sup>-1</sup> for the best structures (*i.e.* leading to H<sub>2</sub> and E<sub>1</sub> with S2B protonated; least for TPSS and most for TPSSh,  $\Delta E_{H_2}$  in Table 2). The only exception is B3LYP, for which the C3 structure is 49 kJ mol<sup>-1</sup> more stable than E<sub>1</sub> + H<sub>2</sub>, *i.e.* an energy that is larger than the entropy gain from H<sub>2</sub> dissociation.

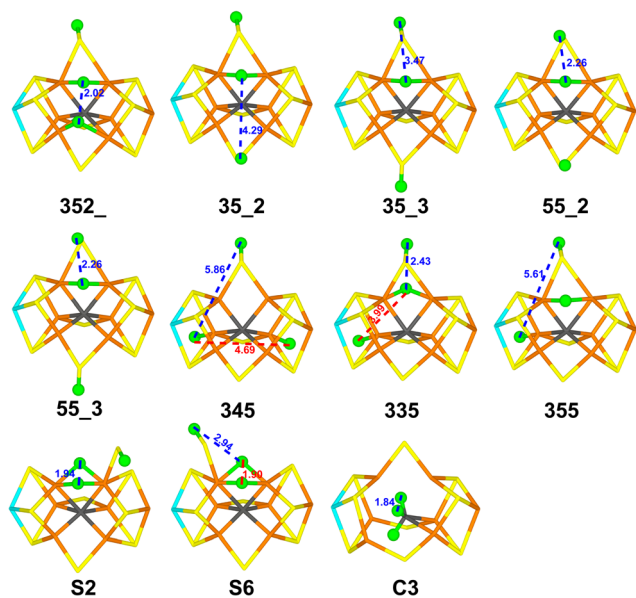


Fig. 4 The eleven considered E<sub>3</sub> structures, showing the structure obtained with TPSS (B3LYP for C3). The labels are explained in the text.

We studied H<sub>2</sub> formation for seven different structures. Interestingly, the activation barrier for the reactions depends mainly on what types of H atoms are involved. Connecting two Fe-bound hydride ions give small barriers. The two hydride ions in the S6 structure (at a H–H distance of 1.90 Å) can be connected with an activation energy of only 57 (TPSS) or 29 (TPSSh) kJ mol<sup>-1</sup>. The reason for the large difference between the two functionals is that the reaction is much more exothermic with TPSSh than with TPSS (42 and 5 kJ mol<sup>-1</sup>), because the product state contains S2B dissociated from Fe2 (and H<sub>2</sub> bound to Fe2). The transition state is later for TPSS (the H–H distances are 1.1 and 1.3 Å, respectively). Likewise, the barrier to connect the two Fe2/6 and Fe3/7 bridging hydride ions in the 352\_ structure, at an initial distance of 2.02 Å, is only 34–39 kJ mol<sup>-1</sup>.

More complicated reactions involving two hydride ions also give relatively low barriers. The Fe2/6 and Fe5 hydride ions in the 335 structure are initially at a distance of 3.91–3.99 Å. However, they can form H<sub>2</sub> by first moving the Fe2/6 hydride ion also to Fe5 (in the *endo* position) (*i.e.* almost bridging to Fe4) and then connect the two hydride ions. The first step has a barrier of 46–55 kJ mol<sup>-1</sup>, whereas the second step is facile with a barrier of only 30–31 kJ mol<sup>-1</sup>. Likewise, the two terminal hydride ions on Fe4 and Fe5 in the 345 structure, initially 5.9 Å apart, can be connected *via* an intermediate with the Fe5 hydride ion moved to S5A and a net barrier of 52 kJ mol<sup>-1</sup> with TPSS and only 29 kJ mol<sup>-1</sup> for TPSSh (in both cases for the first step).

On the other hand, reactions involving a proton and a hydride ion have appreciably higher activation energies. The proton on S2B and the hydride ion bridging Fe2/6 in the 55\_2 structure are initially at a distance of 2.26–2.27 Å. They can form H<sub>2</sub> *via* an activation barrier of 75 (TPSS) to 115 kJ mol<sup>-1</sup> (TPSSh). Likewise, the same two H atoms in the 335 structure (on the other side of the cluster), with an initial distance of 2.43–2.47 Å, can be connected with a barrier of 101–110 kJ mol<sup>-1</sup>. The same applies to the proton on S2B and the closest Fe2/6 hydride ion in the S6 structure (initially 2.92–2.94 Å apart). They can be connected passing a barrier of 118 (TPSS) or 86 kJ mol<sup>-1</sup> (TPSSh).

However, we failed to find any reaction of the two close protons on the central carbide in the C3 structure with both B3LYP and TPSSh. Although the two protons are only 1.76 Å apart at the start, the reaction was monotonously uphill to over 200 kJ mol<sup>-1</sup>.

We also studied some proton-transfer reactions within the cluster. For example, the Fe hydride ion bridging Fe3/7 could be moved to S5A in the 352\_ structure (forming the 35\_2 structure) with a barrier of 53 (TPSS) or 26 kJ mol<sup>-1</sup> (TPSSh). Again, the reason for the lower barrier with TPSSh is that the reaction is more exothermic with that functional.

Among the product structures, the one started from the 345 structure was most stable, because it resulted in a E<sub>1</sub> structure with a proton on S2B(3) and H<sub>2</sub> in the second coordination sphere. It was 61–114 kJ mol<sup>-1</sup> more stable than the best E<sub>3</sub> state with the TPSS, r<sup>2</sup>SCAN and TPSSh functionals, but 42 kJ mol<sup>-1</sup> less stable than the C3 structure with B3LYP. Three structures had H<sub>2</sub> coordinated to the cluster (either to Fe2 or Fe7), but these



**Table 2** Structures and reactions within the  $E_3$  state, listing the structure (Struct), the positions of the three added H atoms (H1, H2 and H3), the BS state, the H–H distance (Å), the relative energy ( $\Delta E$ ), the  $H_2$  dissociation energy ( $\Delta E_{H_2}$ ) relative the  $E_1$  state and  $H_2$  in a COSMO solvent, and the activation energy for  $H_2$  formation ( $\Delta E^\ddagger$ ; all energies in  $\text{kJ mol}^{-1}$ ). For the 335 and S6 structures, two reactions were studied, connecting either a hydride ion and a proton (HP) or two hydride ions (HH; the two H atoms involved in the reactions are marked in bold face). The lower part of the table shows the products after the  $H_2$ -formation reactions, labelled after the starting  $E_3$  structure and reaction

Struct.	H1	H2	H3	BS	TPSS				$r^2\text{SCAN}$		TPSSh				B3LYP	
					H–H	$\Delta E$	$\Delta E_{H_2}$	$\Delta E^\ddagger$	$\Delta E$	$\Delta E_{H_2}$	H–H	$\Delta E$	$\Delta E_{H_2}$	$\Delta E^\ddagger$	$\Delta E$	$\Delta E_{H_2}$
352_	S2B(3)	<b>Fe2/6(5)</b>	<b>Fe3/7(2)</b>	147	2.02	57	−116	39	77	−169	2.03	62	−170	34	265	−216
35_2	S2B(3)	<b>Fe2/6(5)</b>	<b>S5A(2)</b>	147	4.29	55	−115	136	56	−148	4.26	32	−139	124	178	−129
35_3	S2B(3)	Fe2/6(5)	S5A(3)	147	3.47	46	−105		45	−137	3.50	21	−128		187	−138
55_2	<b>S2B(5)</b>	<b>Fe2/6(5)</b>	S5A(2)	147	2.26	74	−133	75	77	−168	2.27	51	−158	115	212	−163
55_3	S2B(5)	Fe2/6(5)	S5A(3)	147	2.26	63	−122		65	−156	2.26	40	−147		206	−157
345	<b>S2B(3)</b>	<b>Fe4</b>	Fe5	147	5.86	68	−127	52	58	−150	5.91	58	−165	29	248	−199
335 HP	<b>S2B(3)</b>	<b>Fe2/6(3)</b>	Fe5	147	2.43	61	−120	101	69	−161	2.47	56	−163	110	258	−209
HH		<b>Fe2/6(3)</b>	<b>Fe5</b>		3.99			55			3.91			46		
355	S2B(3)	Fe2/6(5)	Fe5	147	5.61	55	−115		58	−150	5.65	44	−152		242	−193
S2	S2B(H2)	Fe2/6(3)	Fe2/6(5)	147	1.94	59	−118		67	−158	1.93	52	−159		263	−214
S6 HP	S2B(H6)	<b>Fe2/6(3)</b>	<b>Fe2/6(5)</b>	147	1.90	0	−72	118	0	−91	1.90	0	−107	86	195	−146
HH	<b>S2B(H6)</b>	<b>Fe2/6(3)</b>			2.94		−59	57			2.92			29		
C3	C2367	C2456	C3457	147	1.84	189	−248		141	−233	1.80	4 <sup>a</sup>	−111		0	49 <sup>b</sup>
Product states = $E_1 + H_2$																
352_	S2B(3)	$H_2$ on Fe7		147	0.85	77	−136	139	104	−195	0.84	74	−181	187	233	−184
55_2	S5A(2)	$H_2$ dissociated		147	0.76	31	−90	92	12	−103	0.76	−1	−107	113	151	−102
345	S2B(3)	$H_2$ dissociated		147	0.77	−61	2	0	−109	18	0.76	−114	6	0	42	7
335 HP	Fe5	$H_2$ dissociated		147	0.76	−25	−34	37	−55	−36	0.76	−46	−61	68	134	−85
335 HH	S2B(3)	$H_2$ dissociated		147	0.76	−49	−11	13	−97	5	0.76	−101	−6	13	56	−7
S6 HP	Fe2,6(5)	$H_2$ on Fe2 <sup>c</sup>		147	0.79	49	−108	110	28	−119	0.78	34	−142	148	222	−173
S6 HH	S2B(H6)	$H_2$ on Fe2 <sup>d</sup>		147	0.76	9	−68	70	−38	−54	0.77	−42	−65	71	115	−67

<sup>a</sup> BS-136. <sup>b</sup> Barrier > 250  $\text{kJ mol}^{-1}$ . <sup>c</sup> S2B dissociated from Fe2. <sup>d</sup> Protonated S2B dissociated from Fe2.

structures were at least 70–73  $\text{kJ mol}^{-1}$  less stable than the best structure with  $H_2$  dissociated. It should be noted, however, that we have not made any systematic investigation of  $H_2$ -bound (or  $H_2$ -dissociated) structures.

## $H_2$ dissociation from the $E_4$ state

Finally, we studied  $H_2$  formation for the  $E_4$  state. We studied 24 reactions, starting from 14 different structures, described in Table 3 and in Fig. 5. Most of the structures are of two different types. The first have two protons on S2B and S5A and two hydride ions bridging Fe2/6 and Fe3/7, as suggested by Hoffman and coworkers.<sup>38</sup> As for the  $E_3$  structures, they are named according to the direction of the four H atoms (towards S3A, S2B or S5A), given by a number in the order S2B–Fe2/6–Fe3/7–S5A, e.g. 5522 (cf. Fig. 5). We also studied two structures with S2B dissociated from Fe2 (3323H6 and 3523H6). The second group is related to the S2 and S6 structures for  $E_3$ . They also have protons on S2B and S5A, and two hydride ions, but both hydride ions bridge Fe2 and Fe6, and S2B has dissociated from either Fe2 (S6) or Fe6 (S2). Both structures have two local minima depending on the direction of the proton on S2B (cf. Table 3). In addition, we studied two differing structures: 3H has a proton on S2B and three hydride ions on Fe5, Fe6 and bridging Fe2/6. C3 has three protons on the central carbide and one on S2B.

The relative stabilities of the various  $E_4$  states were discussed in a previous study,<sup>32</sup> showing that S61 is most stable with TPSS, TPSSh and  $r^2\text{SCAN}$ , but C3 with B3LYP (which is 233  $\text{kJ mol}^{-1}$  more stable than S61 with this functional, whereas C3 is 192,

146 and 1  $\text{kJ mol}^{-1}$  less stable than S61 with TPSS, TPSSh and  $r^2\text{SCAN}$ , respectively). However, with TPSS, several Hoffman-type structures are competitive, in particular 3323, which is only 3  $\text{kJ mol}^{-1}$  less stable than S61 (27 and 11  $\text{kJ mol}^{-1}$  less stable with  $r^2\text{SCAN}$  and TPSSh).

With the TPSS, TPSSh and  $r^2\text{SCAN}$  functionals, all studied  $E_4$  structures are less stable than the best  $E_2$  structure and  $H_2$  in a COSMO solvent (i.e.  $\Delta E_{H_2}$  in Table 3) by at least 72, 103 and 95  $\text{kJ mol}^{-1}$ , respectively. On the other hand, the C3 structure is 3  $\text{kJ mol}^{-1}$  more stable than the dissociated state with B3LYP. Thus, we can again conclude that formation and dissociation of  $H_2$  from the FeMo cluster is highly thermodynamically favourable and should be kinetically controlled. Therefore, we performed a thorough investigation of the formation of  $H_2$  from all pairs of H atoms on the same face of the FeMo cluster in 14 different starting structures.

The barriers of all 24 studied reactions are collected in Table 3. The reactions can be divided into five groups. The smallest barrier, 15–25  $\text{kJ mol}^{-1}$ , is found for the reaction of two hydride ions bound to the same Fe6 ion, one terminal and the other bridging to Fe2 in the 3H structure. This gives an initial H–H distance of 2.30–2.40 Å. Likewise, reactions from the S61 and S64 structures, where the two hydride ions both bridge Fe2 and Fe6 also give quite small barriers of 34–47  $\text{kJ mol}^{-1}$ . In the starting structure, the two hydride ions are only 1.74–1.87 Å apart.

Five reactions have barriers of 59–72  $\text{kJ mol}^{-1}$  with TPSS and 48–81  $\text{kJ mol}^{-1}$  with TPSSh. They all involve reactions between a proton on S2B and hydride ion bridging Fe2 and Fe6. They have initial H–H distances of 2.24–2.37 Å, irrespectively of



**Table 3** Structures and reactions within the E<sub>4</sub> state, listing the structure (Struct), the positions of the four added H atoms (H1, H2, H3 and H4), the BS state, the H–H distance (Å), the relative energy (ΔE), the H<sub>2</sub> dissociation energy (ΔE<sub>H<sub>2</sub></sub>) relative the E<sub>0</sub> state and H<sub>2</sub> in a COSMO solvent, and the activation energy for H<sub>2</sub> formation (ΔE<sup>‡</sup>; all energies in kJ mol<sup>−1</sup>). The two H atoms involved in the reaction are marked in bold face. The lower part of the table shows the products after the H<sub>2</sub>-formation reactions, labelled after the starting E<sub>3</sub> structure and reaction

Structure	H1	H2	H3	H4	TPSS					r <sup>2</sup> SCAN				TPSSh					B3LYP		
					BS	H-H	ΔE	ΔE <sub>H<sub>2</sub></sub>	ΔE <sup>‡</sup>	BS	ΔE	ΔE <sub>H<sub>2</sub></sub>	BS	H-H	ΔE	ΔE <sub>H<sub>2</sub></sub>	ΔE <sup>‡</sup>	BS	ΔE	ΔE <sub>H<sub>2</sub></sub>	
3H	S2B(3)	<b>Fe2/6(3)</b>	<b>Fe5</b>	Fe6	14	4.02	40	−112	75	14	125	−228	147	3.90	112	−207	72	147	333	−330	
		<b>Fe2/6(3)</b>	<b>Fe6</b>			2.40			25					2.30			15				
	<b>S2B(3)</b>	<b>Fe2/6(3)</b>				2.39			59					2.39			57				
3322	<b>S2B(3)</b>	<b>Fe2/6(3)</b>	Fe3/7(2)	S5A(2)	14	2.36	15	−87	70	147	52	−156	147	2.57	39	−134	80	147	292	−289	
			<b>Fe3/7(2)</b>	<b>S5A(2)</b>		2.55			101					2.48			105				
3323	<b>S2B(3)</b>	<b>Fe2/6(3)</b>	Fe3/7(2)	S5A(3)	14	2.37	3	−75	72	135	27	−131	135	2.45	11	−107	81	135	233	−230	
3323H6	<b>S2B(H6S)</b>	<b>Fe2/6(3)</b>	Fe3/7(2)	S5A(3)	147	2.37	39	−111	76	147	44	−147	147	2.36	49	−145	88	147	313	−311	
		<b>Fe2/6(3)</b>	<b>Fe3/7(2)</b>			3.24			92					3.09			56				
3522	S2B(3)	<b>Fe2/6(5)</b>	<b>Fe3/7(2)</b>	S5A(2)	14	2.04	24	−96	75	14	76	−179	14	2.09	48	−143	53	147	266	−264	
			<b>Fe3/7(2)</b>	<b>S5A(2)</b>		2.48			99					2.51			74				
3523	S2B(3)	<b>Fe2/6(5)</b>	<b>Fe3/7(2)</b>	S5A(3)	14	2.08	14	−86	80	147	25	−129	135	2.26	18	−113	43	346	192	−189	
3523H6	<b>S2B(H6S)</b>	<b>Fe2/6(5)</b>	Fe3/7(2)	S5A(3)	147	2.36	39	−111	77	147	44	−147	147	2.35	49	−145	88	147	293	−291	
		<b>Fe2/6(5)</b>	<b>Fe3/7(2)</b>			3.16			91					3.09			56				
5322	S2B(5)	Fe2/6(3)	<b>Fe3/7(2)</b>	<b>S5A(2)</b>	14	2.53	22	−93	98	147	59	−162	147	2.56	48	−143	102	147	305	−303	
	<b>S2B(5)</b>		<b>Fe3/7(2)</b>			2.96			81					2.97			72				
5323	<b>S2B(5)</b>	Fe2/6(3)	<b>Fe3/7(2)</b>	S5A(3)	14	2.77	11	−83	78	147	45	−148	147	3.09	37	−132	67	147	296	−293	
5522	<b>S2B(5)</b>	<b>Fe2/6(5)</b>	Fe3/7(2)	S5A(2)	14	2.24	41	−112	61	147	59	−162	147	2.32	51	−147	49	147	305	−303	
		<b>Fe2/6(5)</b>	<b>Fe3/7(2)</b>			2.09			85					2.17			60				
			<b>Fe3/7(2)</b>	<b>S5A(2)</b>		2.51			102					2.51			77				
5523	<b>S2B(5)</b>	<b>Fe2/6(5)</b>	Fe3/7(2)	S5A(3)	14	2.25	30	−101	63	147	43	−146	147	2.32	40	−136	48	147	296	−294	
		<b>Fe2/6(5)</b>	<b>Fe3/7(2)</b>			2.13			84					2.19			46				
S2	S2B(H2)	Fe2/6(3)	Fe2/6(5)	S5A(3)	147	1.88	54	−126		147	79	−182	147	1.86	56	−152		147	293	−290	
S64	S2B(H64)	<b>Fe2/6(3)</b>	<b>Fe2/6(5)</b>	S5A(3)	147	1.85	1	−72	47	147	29	−132	147	1.87	18	−113	38	147	257	−254	
S61	S2B(H61)	<b>Fe2/6(3)</b>	<b>Fe2/6(5)</b>	S5A(3)	147	1.82	0	−72	42	346	0	−103	157	1.74	0	−95	34	347	229	−226	
C3	S2B(3)	C2367	C2456	C3457	234	1.83	192	−263		346	146	−249	234	1.83	1	−97		234	0	3	
C1	S2B(H6)	Fe2/6	C2367	S5A(3)														346	158	−156	
Product states																					
3H Fe2/6−5	S2B(3)	Fe5			146	0.76	−34	−38		147	−56	−48	147	0.76	−56	−40		147	113	−111	
3H Fe2/6−6	Fe5	Fe6	H <sub>2</sub> on Fe6		14	0.87	80	−152		147	131	−234	147	0.85	132	−227		147	423	−420	
3322	Fe3/7	S5A(2)			147	0.76	−46	−26			−31	−73		0.76	−32	−64			228	−225	
3322	S2B(3)	Fe2/6(3)			147	0.76	−28	−43			−44	−59		0.76	−54	−41			183	−181	
3323	Fe3/7	S5A(3)			147	0.76	−60	−11			−47	−57		0.76	−44	−51			217	−214	
3522	S2B(3)	S5A(2)			147	0.76	21	−93			11	−114		0.76	−11	−84			151	−148	
3522	S2B(3)	Fe2/6(5)			147	0.75	−6	−66			−28	−75		0.75	−34	−61			179	−177	
3523	S2B(3)	S5A(3)			146	0.75	5	−77			−9	−94		0.76	−24	−71			142	−139	
5322	S5A(2)	Fe2/6(3)			235	0.76	41	−112			58	−162		0.75	48	−143			267	−265	
5322	S2B(5)	Fe2/6(3)			147	0.76	−16	−56			−30	−73		0.76	−41	−54			198	−196	
5323	S5A(3)	Fe2/6(3)			146	0.76	47	−119		147	56	−159	147	0.76	36	−132		147	246	−243	
5522	Fe3/7	S5A(2)			147	0.76	1	−73			35	−138		0.75	30	−125			298	−295	
5522	S2B(5)	S5A(2)			147	0.76	41	−112			29	−132		0.77	8	−103			187	−185	
5522	S2B(5)	Fe2/6(5)			147	0.75	7	−79			−12	−91		0.75	−29	−66			195	−192	
5523	Fe3/7	S5A(3)			147	0.76	−10	−61			20	−123		0.75	18	−113			288	−285	
5523	S2B(5)	S5A(3)			146	0.76	21	−93			8	−111		0.76	−6	−89		147	131	−129	
3323H6	Fe3/7(2)	S5A(3)			147	0.75	−34	−38			−44	−59		0.76	−41	−55			220	−217	
3323H6	S2B(5)	S5A(3)			147	0.76	30	−101			17	−121		0.77	−4	−91			178	−176	
3523	Fe3/7(2)	S5A(3)			147	0.75	−67	−5			−44	−59		0.76	−41	−55			255	−252	
3523H6	S2B(5)	S5A(3)			147	0.76	39	−110			17	−121		0.76	−2	−94			172	−170	
S64	S2B(H6M)	S5A(3)	H <sub>2</sub> on Fe2		147	0.94	40	−112			12	−116		0.80	12	−107		346	109	−106	
S61	S2B(H6S)	S5A(3)	H <sub>2</sub> on Fe2		147	0.83	26	−98			9	−113		0.79	−5	−91			84	−82	

whether the two H atoms are on the same side as S5A or S3A. The analogous reaction involving the Fe2/6 hydride and a proton on a half-dissociated S2B give a slightly higher barrier of 76–77 kJ mol<sup>−1</sup> and 88 kJ mol<sup>−1</sup>, respectively. Two reactions also involve the proton on S2B but the hydride ion bridging Fe3 and Fe7. They have slightly larger initial H–H distances, 2.77–3.09 Å and they give slightly larger barriers of 78–81 kJ mol<sup>−1</sup> with TPSS, but lower barriers with TPSSh, 67–72 kJ mol<sup>−1</sup>.

There are four reactions that involve the proton on S5A and the hydride ion bridging Fe3/7. They have initial H–H distances

of 2.48–2.55 Å, but the barriers are appreciably larger, 98–105 kJ mol<sup>−1</sup> (except two barriers with TPSSh, 74–77 kJ mol<sup>−1</sup>). Thus, the barriers depend more on the involved H atoms than on the initial H–H distances.

Finally, seven reactions involve two hydride ions on different Fe ions. Four of them involve hydrides on the Fe2/6 and Fe3/7 pairs, having initial H–H distances of 2.04–2.13 Å. They give barriers of 75–85 kJ mol<sup>−1</sup> with TPSS and 43–60 kJ mol<sup>−1</sup> with TPSSh. Two involve hydrides in the same positions, but with S2B dissociated from Fe2. This gives longer initial distances





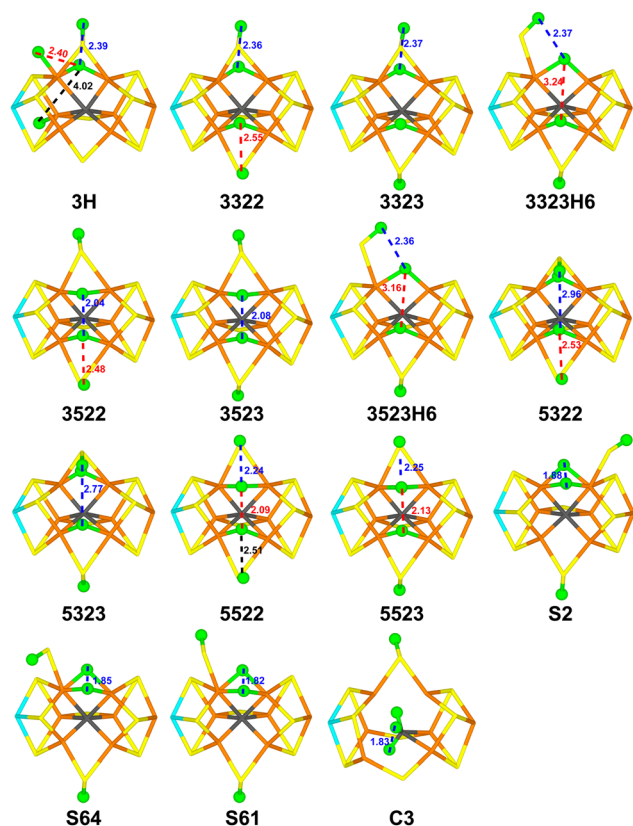


Fig. 5 The 15 considered  $E_4$  structures, showing the structures obtained with TPSS (B3LYP for C3). The labels are explained in the text.

(3.16–3.24 Å) and higher barriers with TPSS (91–92 kJ mol<sup>−1</sup>), but not with TPSSh (56 kJ mol<sup>−1</sup>). The seventh reaction involves hydride ions on Fe2/6 and Fe5 in the 3H complex. In this case, the initial H–H distance is much larger, 4.02 Å. This gives a more complicated reaction, in which the Fe2/6 hydride ion first moves to Fe5, *via* a Fe5/6 bridging position (with a barrier of 72–75 kJ mol<sup>−1</sup>) and then the two hydride ions on the Fe5 ion (with a H–H distance of 2.20 Å) connect with a barrier of 49–58 kJ mol<sup>−1</sup> relative to the starting structure.

We also tried to connect the closest protons on the central carbide in the C3 structure. However, as for the corresponding  $E_2$  and  $E_3$  states, this was not possible – the energy rose monotonically to >170 kJ mol<sup>−1</sup>. On the other hand, it was possible to move the Fe3/7 hydride ion in 3523H6 structure to the central carbide ion. The barrier was only 47 kJ mol<sup>−1</sup> when studied with B3LYP and the product (with protons also on S2B(H6), Fe2/6 and S5A(5)) was 33 kJ mol<sup>−1</sup> more stable than the reactant (and therefore the second-best B3LYP structure), although it is still 158 kJ mol<sup>−1</sup> less stable than the C3 structure. The corresponding reaction with TPSSh was not possible, mainly owing to the low stability of the product, but also to the fact that it was started from the 3523 structure with S2B still bridging and therefore the hydride on Fe2/6 was partly in the way for the movement of the Fe3/7 hydride ion.

In addition, we tried to convert the S61 structure to the 3323 structure. This requires two steps. First, one of the Fe2/6

hydrides needs to move to Fe3/7. This can be done with a barrier of 54–69 kJ mol<sup>−1</sup>. Then, S2B should bind back to Fe2, which can be done with a minimal barrier of 5–7 kJ mol<sup>−1</sup>.

As a result of the study of the H<sub>2</sub>-formation reactions, we obtained 24 different product structures. Most of them have H<sub>2</sub> in the second coordination sphere of the FeMo cluster. The best structure with TPSS has a proton on S5A and a hydride bridging Fe3 and Fe7. With B3LYP, the best structure has two protons on S2B and S5A. With r<sup>2</sup>SCAN and TPSSh, a structure with a proton on S2B and a terminal hydride ion on Fe5 is best. This is quite different from what was observed for the  $E_2$  state without H<sub>2</sub>, indicating that the second-sphere H<sub>2</sub> molecule has a significant influence on the relative energies and reflecting that we have not performed any systematic investigation of this type of complexes. This is also confirmed by the fact that none of the structures is more stable than the fully dissociated  $E_2 + H_2$  state ( $\Delta E_{H_2}$  is −5 to −111 kJ mol<sup>−1</sup> for the best structures with the four DFT methods). In four of the product structures, H<sub>2</sub> coordinates side-on to Fe2 or Fe6. These structures have appreciably larger H–H bond lengths than the other structures (0.80–0.94 Å, compared to 0.75–0.76 Å). The best structure has H<sub>2</sub> bound to Fe2, S2B protonated and bound only to Fe6, and S5A protonated. However, this structure is 24–93 kJ mol<sup>−1</sup> less stable than the best structure with H<sub>2</sub> in the second sphere.

## Conclusions

We have studied the formation of H<sub>2</sub> in the  $E_2$ – $E_4$  states of Mononitrogenase. Even if there are quite some variations between the individual structures and the DFT functionals employed, there are some general trends. The lowest barrier for H<sub>2</sub> formation is obtained when combining two hydride ions, one terminal on Fe6 and one bridging Fe2/6, 15–25 kJ mol<sup>−1</sup>. Combining two hydride ions both bridging Fe2/6 also give low barriers, 29–57 kJ mol<sup>−1</sup>. Combining hydride ions bridging Fe2/6 and Fe3/7, give higher barriers with TPSS, 75–85 kJ mol<sup>−1</sup>, except in the  $E_3$  state (39 kJ mol<sup>−1</sup>). With TPSSh, those barriers are lower, 34–60 kJ mol<sup>−1</sup>. The reaction between a proton and a hydride ion gives similar barriers. With TPSS, combining a proton on S2B and a hydride ion bridging Fe2/6 typically gives lower barriers than combining two hydride ions on Fe2/6 and Fe3/7 or a proton on S5A and a hydride ion bridging Fe3/7. With TPSSh, barriers for two hydride ions are lower and there are smaller differences between the two proton–hydride reactions. Instead, there is some difference between whether the S2B proton and the Fe2/6 hydride ion are on the same side as S5A (lower barrier) or as S3A (higher barrier). For both functionals, it seems that the proton–hydride reactions give a lower barrier as the number of added electrons and protons increase (*i.e.*  $E_2 > E_3 > E_4$ ). In general, TPSSh gives lower barriers than TPSS (by 9 kJ mol<sup>−1</sup> on average), but for proton–hydride reactions, the opposite is often true.

We have also studied some other reactions, moving around the H atoms within the FeMo cluster. In agreement with previous studies of proton transfers in the FeMo cluster during the later ( $E_4$ – $E_8$ ) steps of the reaction mechanism,<sup>60</sup> we find



that individual barriers are rather small, 5–69 kJ mol<sup>-1</sup>. The calculations show that a proton on S2B can rotate rather freely, either moving from the S2B(3) to the S2B(5) side (55–62 kJ mol<sup>-1</sup>) when S2B is bridging Fe2/6 or rotating around the Fe6–S2B (12–17 kJ mol<sup>-1</sup>) axis when it is dissociated from Fe6. The dissociation of S2B from Fe2 also has a low barrier (35–39 kJ mol<sup>-1</sup>). In fact, it is also possible to move a Fe3/7 hydride ion to S5A (26–53 kJ mol<sup>-1</sup>) or to move a bridging hydride ion from Fe2/6 to Fe3/7 (54–69 kJ mol<sup>-1</sup>). A hydride ion can move to the central carbide with B3LYP (47 kJ mol<sup>-1</sup>), but only in the E<sub>4</sub> state and if the starting structure is appropriate. This shows that the various isomers of the E<sub>n</sub> states can interconvert rather freely. Therefore, it is unlikely that the FeMo cluster may avoid unwanted side reactions by placing the H atoms on different faces of the FeMo cluster. Likewise, it seems impossible to avoid the most stable structures for each E<sub>n</sub> state, *i.e.* to stabilise metastable states by kinetic pathways and barriers.

Finally, we discuss the implications of the current calculations on the reaction mechanism of nitrogenase. From a functional point of view, it is clear that the enzyme should avoid the formation of H<sub>2</sub> before N<sub>2</sub> binds, *i.e.* at least for the E<sub>2</sub> and E<sub>3</sub> states. For the E<sub>2</sub> state, B33 is the most stable structure with TPSS. Formation of H<sub>2</sub> from this state has an activation barrier of 86–91 kJ mol<sup>-1</sup>. This corresponds to a rate of 0.0008–0.0072 s<sup>-1</sup> (3–26 h<sup>-1</sup>; using classical transition-state theory with a pre-exponential factor of 6.2 × 10<sup>12</sup> s<sup>-1</sup>), which is smaller than the turnover rate of the enzyme 1–5 s<sup>-1</sup>.<sup>2,85</sup> Thus, the protein should be able to avoid this side reaction if the electron flow is proper, but the rate constant is somewhat smaller than what has been estimated from kinetic measurements, 0.2 s<sup>-1</sup>,<sup>85</sup> corresponding to 77 kJ mol<sup>-1</sup>. For the B55 structure, the activation energy for H<sub>2</sub> formation is lower, 51–55 kJ mol<sup>-1</sup>. However, this structure is 33–42 kJ mol<sup>-1</sup> less stable than the best state with TPSS or TPSSh, giving net barriers of 84–97 kJ mol<sup>-1</sup>, corresponding to rates of 0.2–65 h<sup>-1</sup>, still much lower than the turnover rate. For the H6 structure, which is the most stable structure with TPSSh and r<sup>2</sup>SCAN, the activation barrier for H<sub>2</sub> formation is quite high, 79–104 kJ mol<sup>-1</sup>. This corresponds to rates of 0.13–5 × 10<sup>-6</sup> s<sup>-1</sup> (0.02–460 h<sup>-1</sup>), which are less than the turnover rate of the enzyme. For the best structure with B3LYP, C2, no H<sub>2</sub> formation could be obtained. Thus, we can conclude that H<sub>2</sub> formation does not seem to be any serious problem at the E<sub>2</sub> level of the protein.

Our calculated activation barrier for the H6 structure of E<sub>2</sub> is similar to that reported by Thorhallsson and Bjornsson, 86 kJ mol<sup>-1</sup>, with TPSSh.<sup>33</sup> On the other hand, our barrier for the B55 structure (51 kJ mol<sup>-1</sup>) is somewhat larger than that reported by Khadka and coworkers, 29 kJ mol<sup>-1</sup>.<sup>52</sup> This might be caused by the difference in DFT methods (TPSS and BP86) but pure GGA functionals often give similar results for nitrogenase models.<sup>18</sup> It is more likely that the reason for the difference is that Khadka and coworkers used QM-cluster calculations, whereas we have performed QM/MM calculations. In fact, Thorhallsson and Bjornsson reported much lower activation energies with cluster models than QM/MM,<sup>33</sup> indicating that the surrounding enzyme disfavours the H<sub>2</sub> formation.

For the E<sub>3</sub> state, the results are more problematic. The S6 structure, which is preferred with the TPSS, r<sup>2</sup>SCAN and TPSSh functionals, has two hydride ions both bridging Fe2/6, and the barrier of H<sub>2</sub> formation from these two hydrides is small 29–57 kJ mol<sup>-1</sup>, corresponding to 7 × 10<sup>2</sup> to 5 × 10<sup>7</sup> s<sup>-1</sup>, much faster than the turnover of the enzyme. We see no way for the enzyme to avoid this problematic side reaction with the current results. Either the TPSS, r<sup>2</sup>SCAN and TPSSh methods give gravely unreliable results or we have not yet found the proper lowest-energy structure or BS state for E<sub>3</sub>. Alternatively, the B3LYP results are trusted, which indicates that C3 structure is most stable. In our calculations, no H<sub>2</sub> formation is observed from this structure. On the other hand, B3LYP gives very weak N<sub>2</sub> binding in the E<sub>4</sub>,<sup>32</sup> which has led Siegbahn to suggest that four additional reductions are needed before N<sub>2</sub> may bind,<sup>46,83</sup> something that does not find any experimental support.<sup>13</sup>

For the E<sub>4</sub> state, the situation is similar: The best structure with TPSS, r<sup>2</sup>SCAN and TPSSh is S61, with two hydride ions both bridging Fe2/6. These can be connected with a barrier of only 34–47 kJ mol<sup>-1</sup>, corresponding to rates of 5 × 10<sup>4</sup>–7 × 10<sup>6</sup> s<sup>-1</sup>, *i.e.* much faster than the turnover rate of the enzyme. However, with TPSS, the Hoffman-type structures are competitive in stability, in particular 3323, which is only 3 kJ mol<sup>-1</sup> less stable than S61. From this structure, H<sub>2</sub> formation has a higher barrier of 72–81 kJ mol<sup>-1</sup>, *i.e.* similar to the turnover rate of the enzyme. There are other Hoffman-type of complexes with lower barriers (down to 61 kJ mol<sup>-1</sup> with TPSS and 46 kJ mol<sup>-1</sup> with TPSSh), but they are too unstable compared to the best structure so that the net barrier (counted from the best structure) becomes prohibitively high. Finally, the C3 structure is best with B3LYP and competitive with TPSSh, but no H<sub>2</sub> formation could be obtained from this structure. In conclusion, H<sub>2</sub> formation from the best E<sub>4</sub> structures is possible. In this case, it is unclear whether this reaction should take place before or after binding of N<sub>2</sub>, *i.e.* if it should be avoided or not. The results are in accordance with a recent steady-state kinetic model of nitrogenase, indicating that the rate of H<sub>2</sub> formation is much higher from the E<sub>4</sub> state than from E<sub>2</sub>.<sup>85</sup> In future studies, we will study the binding of N<sub>2</sub> to E<sub>4</sub> structures with H<sub>2</sub> and whether the binding of N<sub>2</sub> can be enhanced by the concerted formation or dissociation of H<sub>2</sub>.

## Author contributions

HJ performed all calculations and contributed to the analysis and the writing of the manuscript. UR directed the research, analysed the results and wrote the manuscript.

## Conflicts of interest

There are no conflicts of interest to declare.

## Acknowledgements

This investigation has been supported by grants from the Swedish research council (projects 2018-05003 and 2020-06176) and



from China Scholarship Council. The computations were performed on computer resources provided by the Swedish National Infrastructure for Computing (SNIC) and by the National Academic Infrastructure for Supercomputing in Sweden (NAISS) at Lunarc at Lund University, NSC at Linköping University and HPC2N at Umeå University, partially funded by the Swedish Research Council (grants 2018-05973 and 2022-06725).

## References

- B. K. Burgess and D. J. Lowe, *Chem. Rev.*, 1996, **96**, 2983.
- B. Schmid *et al.*, *Handbook of Metalloproteins*, John Wiley & Sons, Ltd, 2006, p. 1025.
- B. M. Hoffman, *et al.*, *Chem. Rev.*, 2014, **114**, 4041.
- L. C. Seefeldt, *et al.*, *Chem. Rev.*, 2020, **120**, 5082.
- T. Spatzal, *et al.*, *Science*, 2011, **334**, 940.
- J. Kim and D. C. Rees, *Science*, 1992, **257**, 1677.
- O. Einsle, *et al.*, *Science*, 2002, **297**, 1696.
- T. Spatzal, *et al.*, *Science*, 2014, **345**, 1620.
- O. Einsle, *J. Biol. Inorg. Chem.*, 2014, **19**, 737.
- R. N. F. Thorneley, and D. J. Lowe, in *Molybdenum Enzymes*, ed. T. G. Spiro, Wiley, New York, 1985, p. 221.
- Z. Y. Yang, *et al.*, *Proc. Natl. Acad. Sci. U. S. A.*, 2013, **110**, 16327.
- D. Lukoyanov, *et al.*, *J. Am. Chem. Soc.*, 2016, **138**, 10674.
- V. Hoeke, *et al.*, *J. Am. Chem. Soc.*, 2019, **141**, 11984.
- H. Yang, *et al.*, *Inorg. Chem.*, 2018, **57**, 12323.
- R. Y. Igarashi, *et al.*, *J. Am. Chem. Soc.*, 2005, **127**, 6231.
- C. Van Stappen, *et al.*, *Chem. Rev.*, 2020, **120**, 5005.
- I. Dance, *ChemBioChem*, 2020, **21**, 1671.
- L. Cao and U. Ryde, *Phys. Chem. Chem. Phys.*, 2019, **21**, 2480.
- H. Jiang, O. K. G. Svensson and U. Ryde, *Inorg. Chem.*, 2022, **61**, 18067.
- L. Cao, O. Caldararu and U. Ryde, *J. Chem. Theory Comput.*, 2018, **14**, 6653.
- T. Spatzal, *et al.*, *Nat. Commun.*, 2016, **7**, 10902.
- B. Benediktsson and R. Bjornsson, *Inorg. Chem.*, 2017, **56**, 13417.
- R. Bjornsson, F. Neese and S. DeBeer, *Inorg. Chem.*, 2017, **56**, 1470.
- S. J. Yoo, *et al.*, *J. Am. Chem. Soc.*, 2000, **122**, 4926.
- C. Van Stappen, *et al.*, *Inorg. Chem.*, 2019, **58**, 12365.
- C. Van Stappen, *et al.*, *Chem. Sci.*, 2019, **10**, 9807.
- D. A. Lukoyanov, *et al.*, *Inorg. Chem.*, 2022, **61**, 5459.
- H. Jiang, K. J. M. Lundgren and U. Ryde, *Inorg. Chem.*, 2023, **62**(48), 19433–19445.
- J. Tao, *et al.*, *Phys. Rev. Lett.*, 2003, **91**, 146401.
- J. W. Furness, *et al.*, *J. Phys. Chem. Lett.*, 2020, **11**, 8208.
- V. N. Staroverov, *et al.*, *J. Chem. Phys.*, 2003, **119**, 12129.
- H. Jiang and U. Ryde, *Dalton Trans.*, 2023, **52**, 9104.
- A. T. Thorhallsson and R. Bjornsson, *Chem. – Eur. J.*, 2021, **27**, 16788.
- A. D. Becke, *Phys. Rev. A: At., Mol., Opt. Phys.*, 1988, **38**, 3098.
- C. Lee, W. Yang and R. G. Parr, *Phys. Rev. B: Condens. Matter Mater. Phys.*, 1988, **37**, 785.
- A. D. Becke, *J. Chem. Phys.*, 1993, **98**, 1372.
- Y. Pang and R. Bjornsson, *Phys. Chem. Chem. Phys.*, 2023, **25**, 21020.
- S. Raugei, L. C. Seefeldt and B. M. Hoffman, *Proc. Natl. Acad. Sci. U. S. A.*, 2018, **115**, 10521.
- L. Cao and U. Ryde, *J. Chem. Theory Comput.*, 2020, **16**, 1936.
- A. T. Thorhallsson, B. Benediktsson and R. Bjornsson, *Chem. Sci.*, 2019, **10**, 11110.
- P. E. M. Siegbahn, *J. Am. Chem. Soc.*, 2016, **138**, 10485.
- P. E. M. Siegbahn, *J. Comput. Chem.*, 2018, **39**, 743.
- J. B. Varley, *et al.*, *Phys. Chem. Chem. Phys.*, 2015, **17**, 29541.
- M. Rohde, *et al.*, *Biochemistry*, 2018, **57**, 5497.
- W.-L. Li, *et al.*, *Chem. Catal.*, 2023, **3**(7), 100662.
- P. E. M. Siegbahn, *Phys. Chem. Chem. Phys.*, 2023, **25**, 23602.
- D. Sippel, *et al.*, *Science*, 2018, **359**, 1484.
- W. Kang, *et al.*, *Science*, 2020, **368**, 1381.
- I. Dance, *J. Am. Chem. Soc.*, 2007, **129**, 1076.
- I. Dance, *Z. Anorg. Allg. Chem.*, 2015, **641**, 91.
- I. Dance, *Dalton Trans.*, 2021, **50**, 18212.
- N. Khadka, *et al.*, *J. Am. Chem. Soc.*, 2017, **139**, 13518.
- L. Cao, O. Caldararu and U. Ryde, *J. Phys. Chem. B*, 2017, **121**, 8242.
- B. M. Barney, *et al.*, *Biochemistry*, 2007, **46**, 6784.
- J. A. Maier, *et al.*, *J. Chem. Theory Comput.*, 2015, **11**, 3696.
- W. L. Jorgensen, *et al.*, *J. Chem. Phys.*, 1983, **79**, 926.
- L. Hu and U. Ryde, *J. Chem. Theory Comput.*, 2011, **7**, 2452.
- C. I. Bayly, *et al.*, *J. Phys. Chem.*, 1993, **97**, 10269.
- F. Furche, *et al.*, *Wiley Interdiscip. Rev.: Comput. Mol. Sci.*, 2014, **4**, 91.
- H. Jiang, *et al.*, *Angew. Chem., Int. Ed.*, 2022, **61**, e202208544.
- B. Benediktsson and R. Bjornsson, *J. Chem. Theory Comput.*, 2022, **18**, 1437.
- A. Schäfer, H. Horn and R. Ahlrichs, *J. Chem. Phys.*, 1992, **97**, 2571.
- K. Eichkorn, *et al.*, *Chem. Phys. Lett.*, 1995, **240**, 283.
- K. Eichkorn, *et al.*, *Theor. Chem. Acc.*, 1997, **97**, 119.
- E. Caldeweyher, *et al.*, *J. Chem. Phys.*, 2019, **150**, 154122.
- R. Bjornsson, *et al.*, *Chem. Sci.*, 2014, **5**, 3096.
- D. J. Lowe, R. R. Eady and R. N. F. Thorneley, *Biochem. J.*, 1978, **173**, 277.
- D. Lukoyanov, *et al.*, *Inorg. Chem.*, 2014, **53**, 3688.
- D. A. Lukoyanov, *et al.*, *Inorg. Chem.*, 2018, **57**, 6847.
- T. Lovell, *et al.*, *J. Am. Chem. Soc.*, 2001, **123**, 12392.
- L. Cao and U. Ryde, *Int. J. Quantum Chem.*, 2018, **118**, e25627 (16 pages).
- C. Greco, *et al.*, *Int. J. Quantum Chem.*, 2011, **111**, 3949.
- R. K. Szilagyi and M. A. Winslow, *J. Comput. Chem.*, 2006, **27**, 1385.
- L. Cao and U. Ryde, *J. Biol. Inorg. Chem.*, 2020, **25**, 521.
- A. Klamt and G. Schüürmann, *J. Chem. Soc., Perkin Trans. 2*, 1993, 799.
- A. Schäfer, *et al.*, *Phys. Chem. Chem. Phys.*, 2000, **2**, 2187.
- A. Klamt, *et al.*, *J. Phys. Chem. A*, 1998, **102**, 5074.
- U. Ryde, *J. Comput.-Aided Mol. Des.*, 1996, **10**, 153.



- 79 U. Ryde and M. H. M. Olsson, *Int. J. Quantum Chem.*, 2001, **81**, 335.
- 80 N. Reuter, *et al.*, *J. Phys. Chem. A*, 2000, **104**, 1720.
- 81 L. Hu, P. Söderhjelm and U. Ryde, *J. Chem. Theory Comput.*, 2011, **7**, 761.
- 82 L. Cao and U. Ryde, *Front. Chem.*, 2018, **6**, 89.
- 83 P. E. M. Siegbahn, *Phys. Chem. Chem. Phys.*, 2019, **21**, 15747.
- 84 W.-J. Wei and P. E. M. Siegbahn, *Chem. – Eur. J.*, 2022, **28**, e202103745.
- 85 D. F. Harris, A. Badalyan and L. C. Seefeldt, *Biochemistry*, 2022, **61**, 2131.

